Dalton Transactions

Cite this: *Dalton Trans.*, 2012, **41**, 14425

www.rsc.org/dalton

PAPER

Heterodinuclear ruthenium(II)–cobalt(III) complexes as models for a new approach to selective cancer treatment†

Alan M. Downward,[a] Reuben T. Jane,[a] Matthew I. J. Polson,[a] Evan G. Moore[b,c] and Richard M. Hartshorn*[a]

Received 29th August 2012, Accepted 19th September 2012
DOI: 10.1039/c2dt31986a

Heterodinuclear ruthenium(II)–cobalt(III) complexes have been prepared as part of investigations into a new approach to selective cancer treatment. A cobalt(III) centre bearing amine ligands, which serve as models for cytotoxic nitrogen mustard ligands, is connected by a bridging ligand to a ruthenium(II)–polypyridyl moiety. Upon excitation of the ruthenium centre by visible light, electron transfer to the cobalt(III) centre results in reduction to cobalt(II) and consequent release of its ligands. We have synthesised several such structures and demonstrated their ability to release ligands upon excitation of the ruthenium centre by visible light.

Introduction

A key concern in the design of anti-cancer treatments is the selective targeting of cancerous tissue. Many anti-cancer drugs in use today achieve this discrimination by targeting rapidly proliferating cells.[1,2] However, the dosage of such treatments is limited due to the effect on rapidly dividing normal cells, such as bone marrow, hair follicles, and epithelial cells lining the gastrointestinal tract.[1] Physiological differences between tumours and healthy tissue, such as a decrease in pH and oxygen concentration in the former, may offer a superior method of targeting the tumour environment.[3,4]

Denny and co-workers have conducted research into hypoxia-selective treatments consisting of cytotoxic mustard compounds coordinated to a cobalt(III) centre.[5–7] Since coordination to a metal centre utilises the lone pair of electrons on the nitrogen atom, and the cytotoxicity of nitrogen mustard compounds relies on the availability of this lone pair, the toxicity of a nitrogen mustard compound is much lower in such a complex.[5] The *in vivo* reduction from a kinetically inert cobalt(III) complex to a labile cobalt(II) complex would allow for ligand exchange, releasing the cytotoxic nitrogen mustard into the cell. Tumour selectivity might be achieved through reoxidation by molecular oxygen in non-cancerous cells to the inert cobalt(III) oxidation state (Fig. 1).

We are working on a system in which the reduction of the cobalt centre and subsequent release of the cytotoxic mustard compounds may be initiated through the use of light as an external stimulus (Fig. 2).[8] Connection of the cobalt(III) centre to a group which can donate an electron upon excitation by an external light source should allow selective release of the cytotoxic molecules at the tumour site using non-invasive techniques. Light is used as a stimulus in the clinical application of photodynamic therapy, and approaches utilising the photo-induced release of biologically active molecules from transition metal based compounds have also been reported.[9]

Ruthenium polypyridyl complexes have well defined electrochemical and photophysical properties that have seen them utilised in many of areas of research,[10,11] including solar cells,[12]

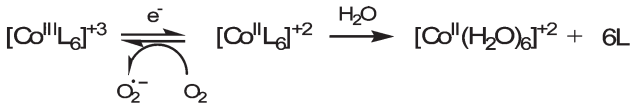

Fig. 1 Reductive activation of cobalt(III) complexes as hypoxia selective cytotoxins.

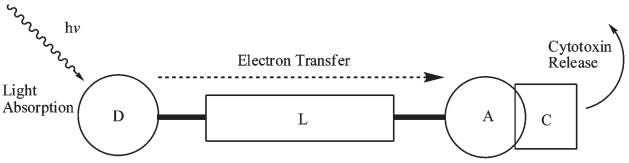

Fig. 2 Schematic of a photo-activated cytotoxin: photo-induced electron transfer from the donor (D) to the acceptor (A) through the bridging ligand (L) results in release of the cytotoxin (C).

[a]*Department of Chemistry, University of Canterbury, Private Bag 4800, Christchurch, New Zealand. E-mail: richard.hartshorn@canterbury.ac.nz; Fax: +64 3 3642110; Tel: +64 3 3642874*
[b]*School of Chemistry, The University of Melbourne, Victoria 3010, Australia*
[c]*School of Chemistry and Molecular Biosciences, University of Queensland, Brisbane, QLD, 4072, Australia. E-mail: egmoore@uq.edu.au; Fax: +61 7 3365 4274; Tel: +61 7 3365 3862*

†Electronic supplementary information (ESI) available: Crystallographic tables, mass spectrometry isotope patterns for Ag^+ titration experiments, voltammograms and UV-vis spectra for mononuclear ruthenium and heterodinuclear ruthenium–cobalt complexes. CCDC 887723 and 887724 for **pytp·$_2$HCl** and **Ru[(bpy)$_2$(pztp)](PF$_6$)$_2$·1.5(CH$_3$CN)** respectively. For ESI and crystallographic data in CIF or other electronic format see DOI: 10.1039/c2dt31986a

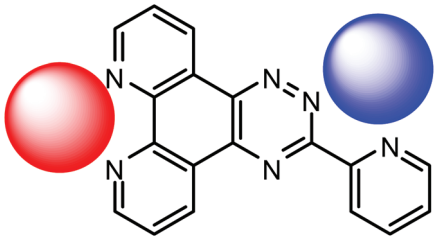

Fig. 3 3-(pyridin-2-yl)-[1,2,4]triazino[5,6-*f*][1,10] phenanthroline (pytp) and its potential metal ion binding domains.

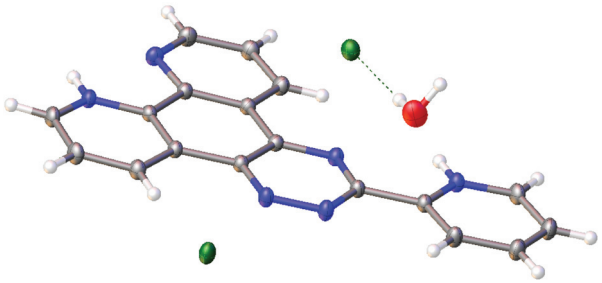

Fig. 4 X-ray crystal structure of pytp·2HCl.

artificial photosynthesis,[13–15] and interactions with DNA and other nucleic acids.[16] The photophysical properties in particular, and the availability of an extensive synthetic chemistry, make ruthenium polypyridyl complexes an excellent class of compounds for use as our electron donor.

The design of the bridging ligand is of utmost importance, as it is this that determines the degree of electronic communication and rate of electron transfer between the metal centres within a dinuclear complex.[17–23] Furthermore, the choice of bridging ligand must be made with consideration to a synthetic route that will allow each metal ion to be placed in the desired binding site of the ligand. For example, we have previously reported the synthesis of functionalised terpyridine derivatives for use as bridging ligands.[24,25] This series was designed with two types of binding domains, differing in number of donors and/or binding configuration, with the purpose of preferentially binding ruthenium(II) at one end, and cobalt(III) at the other.

This paper makes use of Sauer's LEGO system, which provides a synthetic strategy for the formation of a wide range of oligopyridines, in particular to produce ligands with multiple potential metal-binding domains (Fig. 3).[26] While the two metal-binding domains may be very similar in such bridging ligand systems, selectivity of coordination may be achieved by assembly of the ligand with one domain pre-coordinated to the ruthenium(II) centre. Once added, the second binding domain will be available for coordination to a cobalt(III) centre. This approach has been used by the research group of Ji, which has investigated ruthenium(II) complexes of several such ligands, including mononuclear complexes bearing a second binding domain.[27–31] This approach is ideal for assembly of our proposed photoactivated cytotoxin.

Results and discussion

Synthesis of complexes

The ligands 3-(pyridin-2-yl)-[1,2,4]triazino[5,6-*f*][1,10]phenanthroline (pytp) and 3-(pyrazin-2-yl)-[1,2,4]triazino[5,6-*f*][1,10]-phenanthroline (pztp) were synthesised by condensation of 1,10-phenanthroline-5,6-dione with pyridine-2-carbohydrazonamide or pyrazine-2-carbohydrazonamide, respectively, as previously reported by Sauer.[32] These ligands contain two metal-binding domains, and are therefore capable of binding two different metal centres.

Crystals of the dihydrochloride salt of pytp that were suitable for X-ray diffraction studies were obtained by slow evaporation of a solution of the ligand in dilute hydrochloric acid.

The resulting structural refinement shows the ligand to be doubly-protonated, with one proton bound to one of the phenanthroline nitrogen atoms and the other to the pyridyl nitrogen atom (Fig. 4). The molecules pack in sheets with the two chloride ions and one solvent water per molecule close to the mean plane of the ligand. Ligand molecules in different layers are linked by a chain of hydrogen bonds from the protonated pyridyl group, to Cl1, through the water molecule to Cl2 and into the next ligand through the protonated phenanthroline. Although the ligands are flat and lie parallel to each other with a centroid-to-plane distance of 3.317 Å, the molecules have poor overlap, thus π–π interactions appear not to be a stabilising influence.

Attempts to synthesise mononuclear ruthenium(II) complexes by 1 : 1 reaction of the appropriate bridging ligand with $[Ru(bpy)_2Cl_2]\cdot 2H_2O$ gave poor discrimination between the two potential binding sites, as seen by Ji *et al.*[31] ^{1}H NMR spectra of the resulting mixtures were consistent with the presence of both possible mononuclear complexes, along with the diruthenium complex. Well-defined mononuclear ruthenium(II) complexes bearing the bridging ligands pytp and pztp, $[Ru(bpy)_2(pytp)](PF_6)_2$ and $[Ru(bpy)_2(pztp)](PF_6)_2$, respectively, were synthesised using the approach of Ji *et al.* The appropriate carbohydrazonamide was reacted with the pre-coordinated phendione complex, $[Ru(bpy)_2(phendione)](PF_6)_2$, in order to allow selective formation of complexes in which the Ru(II) ion is bound to the phenanthroline-like binding site of the pytp and pztp ligands (Fig. 5).

Crystals of $[Ru(bpy)_2(pztp)](PF_6)_2$ suitable for X-ray diffraction were obtained by the diffusion of diethyl ether into an acetonitrile solution of the complex.

The structure shows that the pztp ligand is bound to the ruthenium centre through the phenanthroline moiety and adopts a planar conformation, similar to that seen in the pytp ligand structure described above. This time however the α-nitrogen of the terminal heterocycle is orientated to form the desired, and more accessible binding domain for the coordination of a second metal centre (Fig. 6).

Heterodinuclear complexes

Although homodinuclear ruthenium(II) complexes of pytp[28] and pztp[31] are known, there are no reports of any heterodinuclear ruthenium(II) complexes of these ligands. Evidence for the ability of the second binding domain to coordinate to a different metal was gathered by monitoring the interaction of the mononuclear ruthenium(II) complexes with silver(I) using ^{1}H NMR spectroscopy.

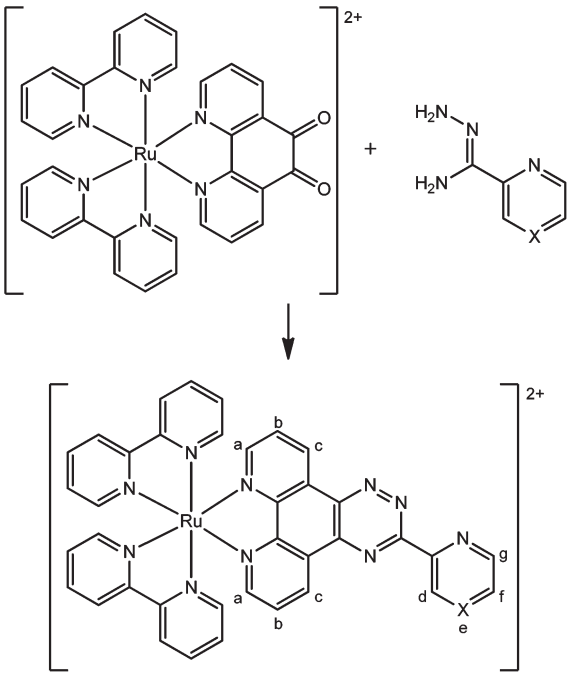

Fig. 5 Synthesis of the ligands pytp (X = CH) and pztp (X = N) on a ruthenium(II) metal centre (counter-ions omitted for clarity). The atomic labels refer to the NMR assignment for $[Ru(bpy)_2(pytp)](PF_6)_2$.

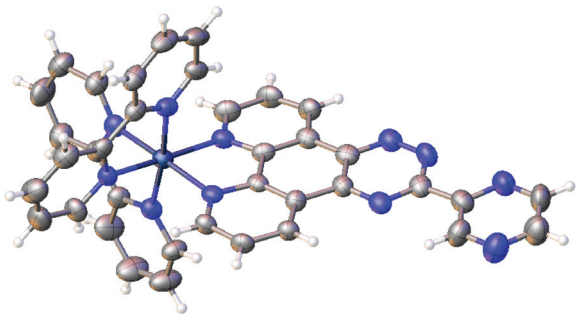

Fig. 6 X-ray crystal structure of $Ru[(bpy)_2(pztp)](PF_6)_2 \cdot 1.5(CH_3CN)$; counter ions and solvent molecules have been omitted for clarity.

$[Ru(bpy)_2(pytp)](PF_6)_2$ was dissolved in acetonitrile-d_3 and $AgClO_4$ added slowly. This resulted in a gradual shift of several of the resonances associated with the pytp ligand, until the ratio of added silver(I) to ruthenium(II) complex was 1 : 1 (Fig. 7). Further addition of silver had minimal affect on the position of the pytp resonances. This is consistent with one to one binding of silver ions, and a fast equilibrium between the bound and unbound state. If the silver was irreversibly bound or the rate of exchange slow on the NMR timescale, then it would be expected that a new set of peaks would appear with the addition of $AgClO_4$. Experiments with salts of zinc(II) or copper(I) ions give similar results, while experiments using non-transition metal salts, $NaClO_4$ and LiCl revealed no evidence for interaction between the ligand and the added metal ions.

Following a silver(I) NMR titration, a portion of the solution was analysed by mass spectrometry. The spectrum showed three

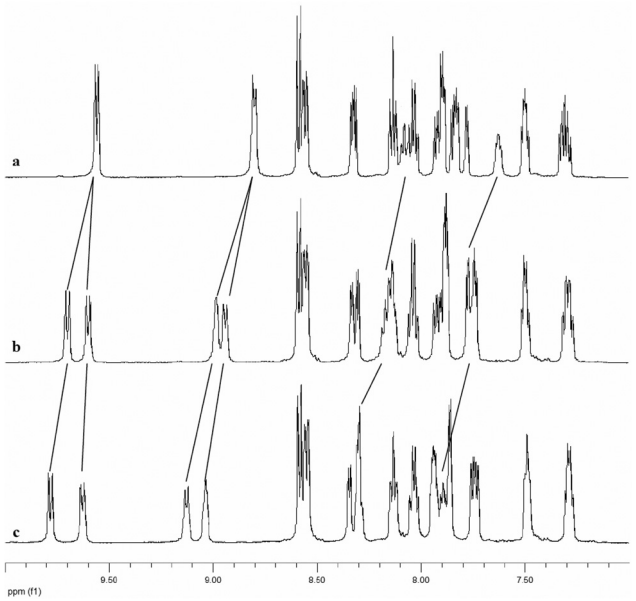

Fig. 7 Aromatic region of ^1H NMR spectra of $[(bpy)_2Ru(pytp)](PF_6)_2$ in CD_3CN with: (a) 0 equivalents of $Ag(ClO_4)$; (b) 0.3 equivalents of $Ag(ClO_4)$; (c) 1 equivalent of $Ag(ClO_4)$.

major isotope patterns that were of interest. These were at *m*/*z* ratios of approximately 362, 466, and 823 and correspond to $[Ru(bpy)_2(pytp)]^{2+}$, $[(bpy)_2Ru(pytp)Ag](ClO_4)^{2+}$ and $[Ru(bpy)_2(pytp)](ClO_4)^{+}$ respectively. This provides further evidence for the binding of silver(I) to the second binding domain of the pytp ligand. Similar results were obtained with $[Ru(bpy)_2(pztp)](PF_6)_2$.

Given that the free binding domains of the mononuclear complexes $[Ru(bpy)_2(pytp)](PF_6)_2$ and $[Ru(bpy)_2(pztp)](PF_6)_2$ are able to coordinate to silver(I) ions, we inferred that they should be suitable for coordination to a cobalt(III) centre. In order to explore this possibility and study the chemistry of the resulting systems, cobalt(III) complexes of the ligands ethane-1,2-diamine (en) and tris(2-aminoethyl)amine (tren) were used. The binding domain of en is similar to that of the bidentate nitrogen mustards that we eventually hope to study, *N*,*N*′-bis(2-chloroethyl)ethane-1,2-diamine and *N*,*N*-bis(2-chloroethyl)ethane-1,2-diamine, while tren, being tetradentate, should be more stable towards substitution.

The Ohno group has prepared heterodinuclear ruthenium(II)–cobalt(III) complexes utilising bidentate and tridentate polypyridyl bridging ligands. This was achieved by heating of a ruthenium(II) complex of the bridging ligand with a cobalt(III) complex bearing exchangeable ligands such as Cl^- or $CF_3SO_3^-$.[33,34] Attempts to form a heterodinuclear complex by heating $[Ru(bpy)_2(pytp)](PF_6)_2$ with $[Co(en)_2Cl_2]Cl$, in aqueous solvents, resulted in products that were unable to be characterised by NMR spectroscopy due to broadening of signals, possibly due to formation of paramagnetic compounds. However, the use of triflate complexes allowed for the synthesis of ruthenium(II)–cobalt(III) heterodinuclear complexes under milder, non-aqueous conditions (Fig. 8).

An acetonitrile solution containing the ruthenium(II) precursor complex, $[Ru(bpy)_2(pytp)]^{2+}$ or $[Ru(bpy)_2(pztp)]^{2+}$, and either

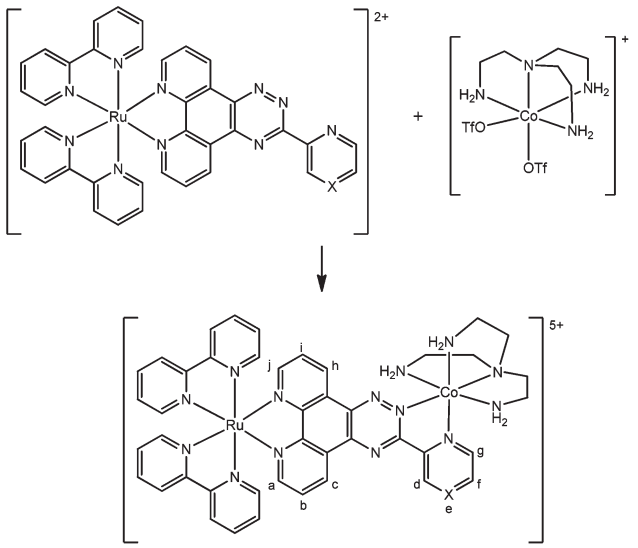

Fig. 8 Synthetic route to $[Ru(bpy)_2(pytp)Co(tren)](PF_6)_5$ in acetonitrile. Counter ions omitted for clarity. The atomic labels refer to the NMR assignment for $[(bpy)_2Ru(pytp)Co(tren)](PF_6)_5$.

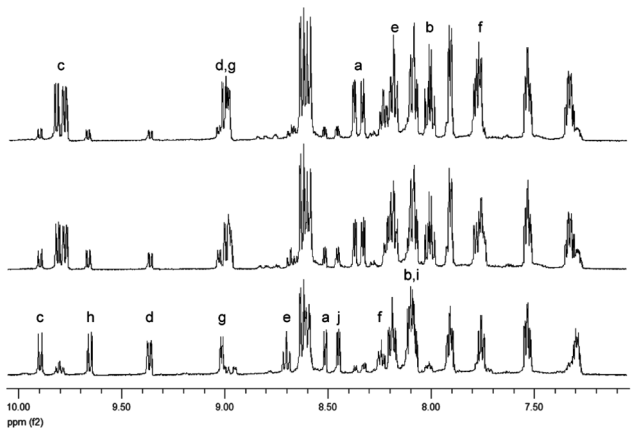

Fig. 9 Aromatic regions of the ^1H NMR spectra taken during the reaction between $[Ru(bpy)_2(pytp)]^{2+}$ and $[Co(tren)(OTf)_2]^+$ in CD_3CN; the top spectrum is primarily $[Ru(bpy)_2(pytp)]^{2+}$ (labelled peaks) while the bottom spectrum is primarily the heterodinuclear complex $[(bpy)_2Ru(pytp)Co(tren)]^{5+}$ (labelled peaks).

$[Co(en)_2(OTf)_2]OTf$ or $[Co(tren)(OTf)_2]OTf$ was stirred at room temperature in a flask protected from light, in order to eliminate the possibility of photoinduced decomposition. The heterodinuclear complexes were then isolated as the PF_6^- salts. While heterodinuclear complexes utilising both pytp and pztp as bridging ligands were synthesised, those containing pztp proved to be unstable in solution, and so discussion from this point focuses on complexes of pytp.

Additional syntheses were conducted on the NMR scale, so that the formation of the product could be monitored by ^1H NMR spectroscopy. The series of spectra shows a decrease in the size of the peaks which are assigned to the starting material, and a corresponding increase in the size of the peaks assigned to the product (Fig. 9).

The UV-vis spectra of both heterodinuclear ruthenium(II)–cobalt(III) complexes are rather similar to those of the mononuclear ruthenium(II) complexes, except that λ_{max} is red-shifted by 6–7 nm, and there is an increase in absorbance in the region below 400 nm.

Electrochemistry

The electrochemistry of $[Ru(bpy)_2(pytp)](PF_6)_2$ and $[(bpy)_2Ru(pytp)Co(tren)](PF_6)_5$ was studied in acetonitrile with $TBABF_4$ as an electrolyte and ferrocene as an internal standard (Table 1).

Both complexes undergo a reversible oxidation process and several reversible or quasi-reversible reduction processes. In both cases, the reversible oxidation is ascribed to the Ru(II)/Ru(III) couple. In the case of the mononuclear complex $[Ru(bpy)_2(pytp)](PF_6)_2$, all the reduction waves can be ascribed to ligand based reductions, with the first wave at −1.22 V assigned to the reduction of the pytp ligand. For the dinuclear complex, the first quasi-reversible reduction wave at −0.26 V can be attributed to the reduction of the cobalt(III) centre to cobalt(II), with the absence of reversibility rationalised as being due to the relatively rapid exchange of the ligands on the metal centre in the cobalt(II) state. In further evidence for this interpretation, larger oxidation currents are observed when scanning to less negative potentials. The second wave, at −0.84 V, is assigned to the reduction of the pytp bridging ligand. Its appearance at a more positive potential, compared with −1.22 V in the mononuclear complex, is attributable to the higher positive charge on the dinuclear complex, making the reduction easier. In both cases, the most negative reduction wave is likely to be due to bipyridine ligand-based reductions.

Luminescence studies

Both the mononuclear complex, $[Ru(bpy)_2(pytp)](PF_6)_2$, and the heterodinuclear complex $[(bpy)_2Ru(pytp)Co(tren)](PF_6)_5$ were shown to luminesce at room temperature, as might be expected for ruthenium(II) polypyridyl complexes.[35] The steady state emission intensity of dinuclear complex was observed to be significantly less than that measured for the mononuclear complex (Fig. 10).

The emission lifetimes of both complexes were calculated by fitting an exponential curve to the observed time-resolved emission data. The mononuclear complex was found to have a lifetime of 212 ns, while the heterodinuclear complex was found to have a lifetime of 72 ns. The quantum yields were calculated, using $[Ru(bpy)_3]Cl_2$ as a standard, with a known quantum yield of 4.2%.[36] From these measurements the mononuclear complex was found to have a quantum yield of 1.11% and the heterodinuclear complex a significantly lower quantum yield of 0.21%,

Table 1 Redox potentials (V, referenced to Fc^+/Fc^0) of $[Ru(bpy)_2(pytp)](PF_6)_2$ (Ru) and $[(bpy)_2Ru(pytp)Co(tren)](PF_6)_5$ (Ru/Co)

	$Ru^{3+/2+}$	$Co^{3+/2+}$	pytp/pytp$^{\cdot-}$	bpy/bpy$^{\cdot-}$
Ru	0.96	—	−1.22	−1.77
Ru/Co	1.00	−0.26	−0.84	−1.64

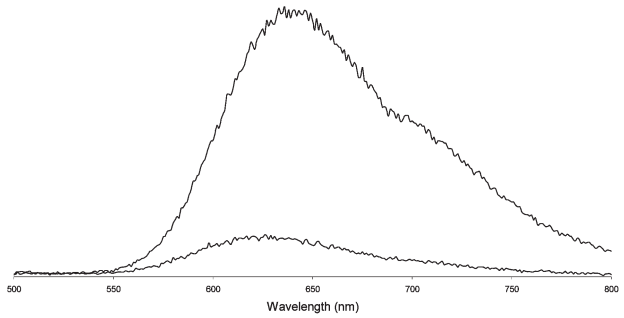

Fig. 10 Comparison of the emission spectra of $[Ru(bpy)_2\ (pytp)]^{2+}$ (upper line) and $[(bpy)_2Ru(pytp)Co(tren)]^{5+}$ (lower line) in CH_3CN.

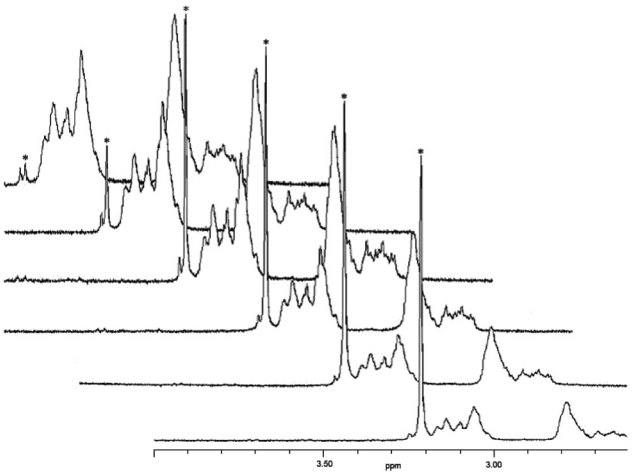

Fig. 11 Photo-induced release of en from $[(bpy)_2Ru(pytp)Co(en)_2]^{5+}$, as seen in aliphatic region of ^1H NMR spectra; the peak associated with the free en molecule is marked (*). Spectra shown were taken after (from top to bottom) 0, 10, 30, 60, 120 and 180 minutes irradiation.

consistent with the differences in steady state emission intensities.

All of these measurement are consistent with coordination of the cobalt(III) metal centre, resulting in a quenching of the excited-state luminescence. Furthermore, if we assume that the ruthenium–polypyridyl-centred radiative and non-radiative decay paths are the same for both complexes, then the rate of electron transfer to the cobalt can be approximated. Using the formula $k_{obs} = k_{rad} + k_{nonrad} + k_{et}$ and assuming that $(k_{rad} + k_{nonrad})$ is equal to k_{obs} of the mononuclear complex, for the heterodinuclear complex, we obtain a value of $9.6 \times 106\ s^{-1}$ for k_{et}.

Photoactivated ligand release

A sample of $[(bpy)_2Ru(pytp)Co(en)_2](PF_6)_5$ was dissolved in 1 : 1 D_2O : acetonitrile-d_3 in a 5 mm NMR tube and irradiated under white light at room temperature. The sample was removed from irradiation at regular intervals in order for ^1H NMR spectra to be recorded. This revealed the appearance and growth over time of a new singlet peak at 3.21 ppm (Fig. 11), which has been assigned to the two methylene groups on the noncoordinated en ligand.

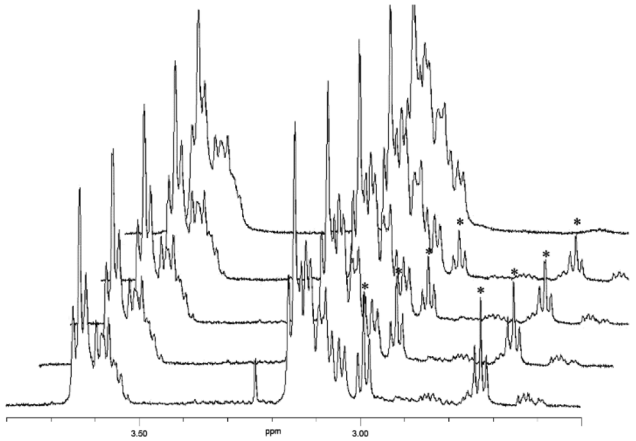

Fig. 12 Photo-induced release of tren from $[(bpy)_2Ru(pytp)Co(tren)]^{5+}$, as seen in aliphatic region of ^1H NMR spectra the peaks associated with the free tren molecule are marked (*). Spectra shown were taken after (from top to bottom) 0, 60, 120, 180 and 240 minutes irradiation.

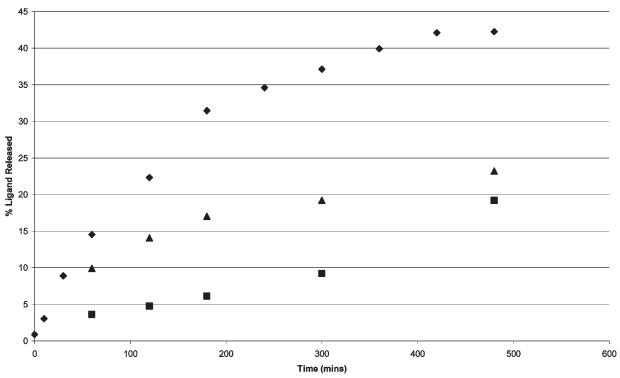

Fig. 13 Difference in rate of ligand release between samples that have undergone freeze–pump–thaw cycles (◆), N_2 bubbling (▲) and no treatment to remove oxygen (■).

Under the same conditions, $[(bpy)_2Ru(pytp)Co(tren)](PF_6)_5$ showed similar behaviour. Two triplets appeared at 2.99 and 2.73 ppm, corresponding to noncoordinated tren in solution (Fig. 12).

The dependence of ligand release on oxygen concentration was examined by repetition of the above experiment utilising $[(bpy)_2Ru(pytp)Co(en)_2](PF_6)_5$ under different levels of solution oxygen concentration. The first sample had no treatment to control its oxygen concentration, the second was bubbled with nitrogen for one minute, and the third was run through a succession of freeze–pump–thaw cycles with nitrogen back-fill to prevent excessive solvent evaporation. The three samples were then irradiated as described above and the amount of en released was estimated by comparison of the integral of the singlet at 3.21 ppm, assigned to noncoordinated en, with the integral of the peak at 9.21 ppm, corresponding to the pytp bridge in the heterodinuclear complex. Plotting the percentage of ligand released as a function of time (Fig. 13) revealed that the ligand was released the fastest in the sample that had been cycled through the freeze–pump–thaw process. The second fastest release of ligand was seen in the nitrogen degassed sample,

which shows that the rate of ligand release is dependent on the concentration of oxygen in solution. This oxygen dependence may be due to reoxidation of the Co(II) centre by dissolved oxygen competing with the exchange of the coordinated ligands for solvent molecules. Other possibilities do exist, however, such as interaction/deactivation of the ruthenium-centred excited state with oxygen. This kind of oxygen-dependent ligand release may enable selective targeting of hypoxic cells, such as those found in poorly vascularised tumours.

Conclusions

Ruthenium(II)–cobalt(III) heterodinuclear complexes utilising pytp and pztp as bridging ligands have been synthesised and characterised. Coordination of the second binding domain to cobalt was found to decrease the luminescence, and shorten the excited state lifetime of the complexes. This is attributed to electron transfer to the cobalt(III) centre providing additional relaxation pathways for the excited state. Furthermore, coordination to cobalt(III) was found to raise the reduction potential of the bridging ligand pytp. Photoactivated release of the ancillary ligands on cobalt(III) has been demonstrated. These results suggest compounds of this kind may be able to be used as a light activated selective cancer treatment, and justify further research utilising nitrogen mustard molecules as the ancillary ligands on the cobalt centre.

Experimental

General experimental

^{1}H and ^{13}C NMR spectra were recorded on Varian UNITY-300 or Varian INOVA-500 spectrometers. Chemical shifts are expressed in parts per million (ppm) on the δ scale and were referenced to residual solvent resonances or to TMS as an internal reference. NMR spectra were assigned using two-dimensional techniques.

High Resolution Electrospray Ionisation Mass Spectra were recorded on a Micromass LCT spectrometer using a probe voltage of 3200 V, an operating temperature of 150 °C and a source temperature of 80 °C.

UV-visible spectra were recorded on a Varian CARY Probe 50 UV-vis spectrophotometer or a Varian CARY 100 UV-vis spectrophotomer.

X-Ray crystal data was collected on a Bruker-Nonius APEX II system using graphite monochromatised Mo Kα (l = 0.71073 Å) radiation at the temperature indicated in the tables that may be found in the ESI.† The data collection, cell determination and data reduction were all performed with the APEX software. All structures had intensities corrected for Lorentz and polarisation effects and for absorption using SAINT. All structures were solved by direct methods using SHELXS and refined on F^2 using all data by full-matrix least squares procedures using SHELXL-97. All non-hydrogen atoms were refined anisotropically, and hydrogen atoms were (C–H) placed in idealised positions with displacement parameters 1.2 and 1.5 times the isotropic equivalent of their carrier carbon atoms or (X–H) located in the electron density map and allowed to refine at a fixed distance (O–H d = 0.82 Å, N–H d = 0.86 Å) with displacement parameters 1.5 times the isotropic equivalent of their carrier atoms.

Steady state absorption measurements were performed using an absorption spectrometer (Cary Bio50, Varian). Steady state emission spectra were acquired with an emission spectrometer (Cary Eclipse, Varian). Quantum yield measurements were performed using the optically dilute method, using $[Ru(bpy)_3]Cl_2$ in aqueous solution as a standard (Φ_{ref} = 4.2%).[36] Time resolved emission lifetime experiments were performed using a nanosecond laser setup. The 355 nm tripled output of a Q-switched Nd:YAG (Continuum NY-61-10, Coherent) was used to drive an OPO system (Casix BBO, Shanghai Uniwave Technologies) which was tuned to 440 nm, and this output was focused on the sample using all quartz optics. Emission was collected perpendicular to the excitation, collimated then refocused onto the entrance port of a 0.3 m triple grating monochromator (SpectraPro 300i, Acton Instruments) for spectral selection at 630 nm. The detector was a PMT tube (R928P, Hamamatsu), the output of which was sampled directly using a 500 MHz digital oscilloscope (TDS520, Tektronix). The instrument response function (IRF) for this setup was measured using scattered excitation to be *ca.* 8 ns at FWHM. Each resulting trace contained at least 1000 data points, and was averaged over 1000 shots. Data analysis was performed using a commercially available software package (Igor, Version 6.1.2.1, Wavemetrics). The quality of the fit was assessed using the reduced chi-squared χ^2 function and by an inspection of the weighted residuals.

All electrochemical measurements were carried out in nitrogen-purged acetonitrile using a computer-controlled Ecochemie Autolab PGSTAT 302 potentiostat. The working electrode was a Pt electrode, the secondary electrode was an Au wire and the pseudo-reference electrode was a silver wire. The reference was set to an internal ferrocene/ferrocinium sample. The concentration of the compounds was about 1 mM. Tetrabutylammonium tetrafluoroborate ($TBABF_4$) was used as supporting electrolyte at a concentration of 0.1 M. Cyclic voltammograms were obtained at scan rates of 100 mV s^{-1}. Half-wave potentials were measured with squarewave voltammetry experiments performed with a step potential of 5 mV, an amplitude of 20 mV, and a frequency of 8 Hz.

Preparations

Pyridine-2-carbohydrazonamide,[37] pyrazine-2-carbohydrazonamide,[37] 3-(pyridin-2-yl)-[1,2,4]triazino[5,6-*f*][1,10]phenanthroline (pytp),[32] 3-(pyrazin-2-yl)-[1,2,4]triazino[5,6-*f*][1,10]phenanthroline (pztp),[32] $[Ru(bpy)_2(phendione)](PF_6)_2$,[38] $[Co(tren)(OTf)_2]OTf$[39] and $[Co(en)_2(OTf)_2]OTf$[39] were prepared according to published procedures.

Single crystals of $C_{18}H_{14}Cl_2N_6O$ were prepared by slow evaporation of an aqueous HCl solution. A suitable crystal was mounted in a perfluoronated oil and placed in the cold stream of a diffractometer.

Crystal structure determination of pytp·2HCl

Crystal data. $C_{18}H_{14}Cl_2N_6O$, M = 401.25, triclinic, a = 8.3203(2) Å, b = 9.8047(3) Å, c = 11.3191(4) Å, α = 112.3820(10)°,

β = 93.764(2)°, γ = 93.041(2)°, V = 848.93(4) Å^3, T = 118(2), space group $P\bar{1}$ (no. 2), Z = 2, μ(MoKα) = 0.406, 22 950 reflections measured, 4919 unique (R_{int} = 0.0863) which were used in all calculations. The final wR_2 was 0.1054 (all data) and R_1 was 0.0366 ($I > 2\sigma(I)$).

[Ru(bpy)$_2$(pytp)](PF$_6$)$_2$. [Ru(bpy)$_2$(pytp)](PF$_6$)$_2$ was synthesised by a modification of the literature method of Zou.[31] A solution of pyridine-2-carbohydrazonamide (0.076 g) in ethanol (5 mL) was added to a solution of [Ru(bpy)$_2$(phendione)](PF$_6$)$_2$·H$_2$O (0.5 g) in acetonitrile (15 mL). The reaction mixture was heated at reflux for one hour, after which it was filtered through celite and the solvent removed under vacuum. The crude product was dissolved in acetonitrile and purified by column chromatography (silica gel, acetonitrile/saturated aqueous KNO$_3$ 7 : 1). The major red band was collected and the product converted to the PF$_6^-$ salt. The solvent was removed under vacuum and the resulting solid dissolved in acetonitrile. The solution was added to vigorously stirred water to precipitate the product which was filtered and washed with 0 °C water, 0 °C ethanol and ether.

Yield 0.30 g (52%). Characterisation data were consistent with those previously reported.[30]

[Ru(bpy)$_2$(pztp)](PF$_6$)$_2$. A solution of pyrazine-2-carbohydrazonamide (0.08 g) in ethanol (5 mL) was added to a solution of [Ru(bpy)$_2$(phendione)](PF$_6$)$_2$·H$_2$O (0.5 g) in acetonitrile (15 mL). The reaction mixture was heated at reflux for one hour, after which it was filtered through celite and the solvent removed under vacuum. The crude product was dissolved in acetonitrile and purified by column chromatography (silica gel, acetonitrile/saturated aqueous KNO$_3$ 7 : 1). The major red band was collected and the product converted to the PF$_6^-$ salt. The solvent was removed under vacuum and the resulting solid dissolved in acetonitrile. The solution was added to vigorously stirred water to precipitate the product which was filtered and washed with 0 °C water, 0 °C ethanol and ether.

Yield 0.24 g (42%). ^{1}H NMR (500 MHz; CD$_3$CN) δ 10.07 (m, 1 H), 9.82 (m, 1 H), 9.72 (m, 1 H), 8.96 (m, 1 H), 8.90 (m, 1 H), 8.54 (m, 4 H), 8.31 (m, 1 H), 8.28 (m, 1 H), 8.13 (m, 2 H), 8.03 (m, 2 H), 7.96 (m, 2 H), 7.85 (m, 2 H), 7.70 (m, 2 H), 7.48 (m, 2 H), 7.27 (m, 2 H). Anal. Calc. for C$_{37}$H$_{25}$F$_{12}$N$_{11}$P$_2$Ru·2H$_2$O (1050.70): C 42.30, H 2.78, N 14.66%; Found: C 42.57, H 2.96, N 14.56. UV-vis (CH$_3$CN): λ_{max}/nm 439.

Single crystals of C$_{40}$H$_{29.5}$F$_{12}$N$_{12.5}$P$_2$Ru were prepared by diffusion of diethyl ether into an acetonitrile. A suitable crystal was mounted in a perfluoronated oil and placed in the cold stream of a diffractometer.

Crystal structure determination of Ru[(bpy)$_2$(pztp)](PF$_6$)$_2$·1.5(CH$_3$CN)

Crystal data. C$_{80}$H$_{59}$F$_{24}$N$_{25}$P$_4$Ru$_2$, M = 2152.54, triclinic, a = 11.8919(7) Å, b = 12.3372(7) Å, c = 15.9036(10) Å, α = 81.000(4)°, β = 77.789(4)°, γ = 66.668(4)°, V = 2087.1(2) Å^3, T = 118(2), space group $P\bar{1}$ (no. 2), Z = 1, μ(MoKα) = 0.556, 34 975 reflections measured, 7380 unique (R_{int} = 0.1090) which were used in all calculations. The final wR_2 was 0.1393 (all data) and R_1 was 0.0559 ($I > 2\sigma(I)$).

[(bpy)$_2$Ru(pytp)Co(tren)](PF$_6$)$_5$. The complexes [Ru(bpy)$_2$(pytp)](PF$_6$)$_2$ (0.0586 g) and [Co(tren)(OTf)$_2$]OTf (0.0377 g) were placed in an aluminium foil-wrapped 25 mL round bottom flask. Acetonitrile (2 mL) was added, the flask stoppered and the solution stirred for 3 hours at room temperature. The product was precipitated out as the PF$_6^-$ salt by drop wise addition to a stirred solution of 3 mL saturated methanolic NH$_4$PF$_6$ diluted in 60 mL water.

Yield 0.0515 g (54%). ^{1}H NMR (500 MHz; CD$_3$CN) δ 9.86 (dd, 1 H, pytp, c), 9.59 (dd, 1 H, pytp, h), 9.33 (dd, 1 H, pytp, d), 8.88 (d, 1 H, pytp, g), 8.69 (t, 1 H, pytp, e), 8.56 (m, 4 H, bpy), 8.49 (dd, 1 H, pytp, a), 8.41 (dd, 1 H, pytp, j), 8.23 (m, 1 H, pytp, f), 8.14 (m, 2 H, bpy), 8.09–8.03 (m, 4 H, pytp (b, i), bpy), 7.85 (m, 2 H, bpy), 7.75 (dd, 1 H, bpy), 7.69 (dd, 1 H, bpy), 7.49 (m, 2 H, bpy), 7.29 (m, 2 H, bpy), 5.30 (br s, 2 H, tren, NH$_2$), 4.64 (m, 2 H, tren), 4.36 (br s, 2 H, tren, NH$_2$), 4.12 (m, 2 H, tren, NH$_2$), 3.64 (m, 4 H, tren), 3.17 (m, 6 H, tren). ^{13}C NMR (75 MHZ; CD$_3$CN) δ 165.17, 159.78 (pytp, a), 158.01 (bpy), 157.82 (pytp, j), 157.79, 155.53 (pytp, g), 154.60, 153.10 (bpy), 152.99 (bpy), 152.47, 151.85, 148.53, 147.13, 144.77 (pytp, e), 139.28 (bpy), 139.26 (bpy), 139.22 (bpy), 139.19 (bpy), 136.41 (pytp, c), 135.05 (pytp, h), 132.96 (pytp, f), 130.38 (pytp, d), 128.68 (bpy), 128.63 (bpy), 128.58 (bpy), 127.81, 127.77, 125.40 (bpy), 65.25 (tren), 61.88 (tren), 47.87 (tren), 44.97 (tren). Anal. Calc. for C$_{44}$H$_{44}$CoF$_{30}$N$_{14}$P$_5$Ru·3CH$_3$OH·2H$_2$O (1785.93): C 31.61, H 3.39, N 10.98%; found: C 31.70, H 3.50, N 11.05%. ESI-MS: m/z (fragment) 1508.6479 ([M − (PF$_6$)]$^+$), 362.2408 ([M − 3(PF$_6$)]$^{3+}$). UV-vis (CH$_3$CN): λ_{max}/nm 206, 253, 285, 444.

[(bpy)$_2$Ru(pytp)Co(en)$_2$](PF$_6$)$_5$. The complexes [Ru(bpy)$_2$(pytp)](PF$_6$)$_2$ (0.0410 g) and [Co(en)$_2$(OTf)$_2$]OTf (0.0263) were placed in an aluminium foil-wrapped 25 mL round bottom flask. Acetonitrile (2 mL) was added, the flask stoppered and the solution stirred for 3 hours at room temperature. The product was precipitated out as the PF$_6^-$ salt by drop wise addition to a stirred solution of 3 mL saturated methanolic NH$_4$PF$_6$ diluted in 60 mL water.

Yield 0.0420 g (64%). ^{1}H NMR (500 MHz; CD$_3$CN) δ 9.85 (m, 1 H), 9.78 (m, 1 H), 9.30 (d, 1 H), 8.83 (d, 1 H), 8.71 (t, 1 H), 8.55 (m, 4 H), 8.47 (m, 1 H), 8.41 (m, 1 H), 8.27 (m, 1 H), 8.14 (m, 2 H), 8.06 (m, 4 H), 7.84 (m, 2 H), 7.74 (t, 1 H), 7.69 (t, 1 H), 7.49 (m, 2 H), 7.30 (m, 2 H), 3.16 (m, 4 H), 3.76 (m, 4 H). Anal. Calc. for C$_{42}$H$_{42}$F$_{30}$N$_{14}$P$_5$CoRu·CH$_3$OH·3H$_2$O (1713.82): C 30.14, H 3.06, N 11.44%; Found: C 30.32, H 3.26, N 11.59%. UV-vis (CH$_3$CN): λ_{max}/nm 445.

[(bpy)$_2$Ru(pztp)Co(en)$_2$](PF$_6$)$_5$. The complexes [Ru(bpy)$_2$(pztp)](PF$_6$)$_2$ (0.0364 g) and [Co(en)$_2$(OTf)$_2$]OTf (0.0246 g) were placed in an aluminium foil-wrapped 25 mL round bottom flask. Acetonitrile (2 mL) was added, the flask stoppered and the solution stirred for 3 hours at room temperature. The product was precipitated out as the PF$_6^-$ salt by drop wise addition to a stirred solution of 3 mL saturated methanolic NH$_4$PF$_6$ diluted in 60 mL water.

Yield 0.0199 g. ^{1}H NMR (500 MHz; CD$_3$CN) δ 9.63 (s, 1 H), 9.17 (d, 1 H), 9.13 (m, 1 H), 8.71 (d, 1 H), 8.31 (t, 1 H), 7.85 (m, 4 H), 7.79 (dd, 1 H), 7.73 (m, 1 H), 7.68 (dd, 1 H), 7.44 (m, 2 H), 7.38–7.31 (m, 4 H), 7.14 (m, 2 H), 6.92 (m, 1 H), 6.78

(m, 2 H), 6.60 (m, 1 H), 6.51 (m, 1 H). UV-vis (CH_3CN): λ_{max}/nm 445.

Acknowledgements

EGM gratefully acknowledges financial support from the Australian Research Council (ARC-DP0879996) and the University of Melbourne.

Notes and references

1 J. M. Brown and A. J. Giaccia, *Cancer Res.*, 1998, **58**, 1408–1416.
2 W. A. Denny, *Eur. J. Med. Chem.*, 2001, **36**, 577–595.
3 T. W. Hambley, *Aust. J. Chem.*, 2008, **61**, 647–653.
4 F. Kratz, I. A. Muller, C. Ryppa and A. Warnecke, *ChemMedChem*, 2008, **3**, 20–53.
5 D. C. Ware, B. D. Palmer, W. R. Wilson and W. A. Denny, *J. Med. Chem.*, 1993, **36**, 1839–1846.
6 D. C. Ware, B. G. Siim, K. G. Robinson, W. A. Denny, P. J. Brothers and G. R. Clark, *Inorg. Chem.*, 1991, **30**, 3750–3757.
7 D. C. Ware, W. R. Wilson, W. A. Denny and C. E. F. Rickard, *J. Chem. Soc., Chem. Commun.*, 1991, 1171–1173.
8 A. M. Downward, E. G. Moore and R. M. Hartshorn, *Chem. Commun.*, 2011, **47**, 7692–7694.
9 U. Schatzschneider, *Eur. J. Inorg. Chem.*, 2010, 1451–1467.
10 S. Campagna, F. Puntoriero, F. Nastasi, G. Bergamini and V. Balzani, *Top. Curr. Chem.*, 2007, **280**, 117–214.
11 J. G. Vos and J. M. Kelly, *Dalton Trans.*, 2006, 4869–4883.
12 A. Hagfeldt, G. Boschloo, L. Sun, L. Kloo and H. Pettersson, *Chem. Rev.*, 2010, **110**, 6595–6663.
13 A. Kimoto, K. Yamauchi, M. Yoshida, S. Masaoka and K. Sakai, *Chem. Commun.*, 2012, **48**, 239–241.
14 M. M. Najafpour, *Chem. Commun.*, 2011, **47**, 11724–11726.
15 Z. Chen, C. Chen, D. R. Weinberg, P. Kang, J. J. Concepcion, D. P. Harrison, M. S. Brookhart and T. J. Meyer, *Chem. Commun.*, 2011, **47**, 12607–12609.
16 F. R. Keene, J. A. Smith and J. G. Collins, *Coord. Chem. Rev.*, 2009, **253**, 2021–2035.
17 S. S. Isied and H. Taube, *J. Am. Chem. Soc.*, 1973, **95**, 8198–8200.
18 H. Fischer, G. M. Tom and H. Taube, *J. Am. Chem. Soc.*, 1976, **98**, 5512–5517.
19 K. Rieder and H. Taube, *J. Am. Chem. Soc.*, 1977, **99**, 7891–7894.
20 S. K. S. Zawacky and H. Taube, *J. Am. Chem. Soc.*, 1981, **103**, 3379–3387.
21 V. Balzani, A. Juris, M. Venturi, S. Campagna and S. Serroni, *Chem. Rev.*, 1996, **96**, 759–833.
22 C. Creutz, *J. Phys. Chem. B*, 2007, **111**, 6713–6717.
23 L. A. A. Deoliveira, L. Dellaciana and A. Haim, *Inorg. Chim. Acta*, 1994, **225**, 129–136.
24 R. Zibaseresht, A. M. Downward and R. M. Hartshorn, *Aust. J. Chem.*, 2010, **63**, 669–679.
25 R. Zibaseresht and R. M. Hartshorn, *Dalton Trans.*, 2005, 3898–3908.
26 G. R. Pabst, O. C. Pfuller and J. Sauer, *Tetrahedron*, 1999, **55**, 8045–8064.
27 H. Chao and L. N. Ji, *Bioinorg. Chem. Appl.*, 2005, **3**, 15–28.
28 H. Chao, Z.-R. Qiu, L.-R. Cai, H. Zhang, X.-Y. Li, K.-S. Wong and L.-N. Ji, *Inorg. Chem.*, 2003, **42**, 8823–8830.
29 H. Chao, G. Yang, G.-Q. Xue, H. Li, H. Zang, I. D. Williams, L.-N. Ji, X.-M. Chen and X.-Y. Li, *J. Chem. Soc., Dalton Trans.*, 2001, 1326–1331.
30 J. Liu, X.-H. Zou, Q.-L. Zhang, W.-J. Mei, J.-Z. Liu and L.-N. Ji, *Metal-Based Drugs*, 2000, **7**, 343–348.
31 X. H. Zou, B. H. Ye, H. Li, J. G. Lin, Y. Xiong and L. N. Ji, *J. Chem. Soc., Dalton Trans.*, 1999, 1423–1428.
32 G. R. Pabst, O. C. Pfuller and J. Sauer, *Tetrahedron Lett.*, 1998, **39**, 8825–8828.
33 H. Torieda, K. Nozaki, A. Yoshimura and T. Ohno, *J. Phys. Chem. A*, 2004, **108**, 4819–4829.
34 H. Torieda, A. Yoshimura, K. Nozaki, S. Sakai and T. Ohno, *J. Phys. Chem. A*, 2002, **106**, 11034–11044.
35 J. P. Sauvage, J. P. Collin, J. C. Chambron, S. Guillerez, C. Coudret, V. Balzani, F. Barigelletti, L. De Cola and L. Flamigni, *Chem. Rev.*, 1994, **94**, 993–1019.
36 J. Van Houten and R. J. Watts, *J. Am. Chem. Soc.*, 1976, **98**, 4853–4858.
37 F. Weldon, L. Hammarström, E. Mukhtar, R. Hage, E. Gunneweg, J. G. Haasnoot, J. Reedijk, W. R. Browne, A. L. Guckian and J. G. Vos, *Inorg. Chem.*, 2004, **43**, 4471–4481.
38 C. A. Goss and H. D. Abruna, *Inorg. Chem.*, 1985, **24**, 4263–4267.
39 N. E. Dixon, W. G. Jackson, G. A. Lawrance and A. M. Sargeson, *Inorg. Synth.*, 1983, **22**, 103–107.

